Electronic Supplementary Information

Active sites provided by surface autocatalytic effect and quantum confinement for stable and efficient photocatalytic hydrogen generation

Ruiming Jia[a§], Qingfeng Gui[b§], Lina Sui[a§], Yan Huang[a], Honggang Lu[a], Hongzhou Dong[a], Shuai Ma[c], Zhixing Gan[a]*, Lifeng Dong[a]*, Liyan Yu[a]*

[a] College of Materials Science and Engineering, Qingdao University of Science and Technology, Qingdao 266042, P. R. China.

[b] College of Naval Architecture and Ocean Engineering, Jiangsu Maritime Institute, Nanjing 211170, P. R. China.

[c] School of Mathematics and Physics, Qingdao University of Science and Technology, Qingdao 266042, P. R. China.

[§] R. Jia. Q. Gui and L. Sui contributed equally to this work.

* E-mail: zxgan@njnu.edu.cn (Z. Gan), donglifeng@qust.edu.cn (L. Dong), liyanyu@qust.edu.cn (L. Yu)

Experimental Section

Materials

Silicon carbide powder (size about 40 nm)，hydrofluoric acid (HF, 40%)，Nafion solution (5 wt.%)，urea, and melamine were purchased from Shanghai Aladdin Biochemical Technology Co., Ltd. Ethanol absolute (≥99.7%), nitric acid and chloroplatinic acid hexahydrate (>99%, $H_2PtCl_6 \cdot H_2O$) were obtained from Sinopharm Group Chemical Reagent Co., Ltd. And all reagents were used without further purification.

The preparation of CN

First, 3 g melamine and 6 g urea were dispersed in 20 mL deionized water, stirred until dissolved and then freeze-dried. Subsequently, the freeze-dried mixture was heated at 550°C for 4 h. The resulting light yellow C_3N_4 nanosheets product was ground to fine powder, which was named as CN. Freeze-drying process can make the product fluffier, which helps to react more fully during thermal polymerization. At high temperature of 550 °C, the urea undergoes the following reaction:

$$6CO(NH_2)_2 = C_3H_6N_6 + 6NH_3\uparrow + 3CO_2\uparrow$$

The gas produced can prevent the accumulation of resulted carbon nitride. Whereas, regarding the melamine, the reaction cannot be described by an exact equation. When the temperature reaches 350 °C, melamine is thermally decomposed to form melamine dimers (melam) through deamination and polycondensation. As the temperature rises to about 390 °C, the melam further deaminates to form 3-s-triazine (melem). At 550 °C, these structural components are poly-condensed to obtain graphite-like layered g-C_3N_4.

The preparation of SiC NCs

SiC nanocrystals (SiC NCs) were prepared by oil bath etching method. Both HNO_3 and HF were used to etch the SiC powders into ultrasmall nanocrystals[1]. During this process, HNO_3 mainly oxidized and dissolved the SiC to form interconnected nanostructure networks. Whereas,

HF was used to remove the silicon oxide formed during the oxidation process. The overall reaction can be described as follows:

$$SiC + 2HNO_3 + 6HF \rightarrow H_2SiF_6 + 2HNO_2 + CO_2 + 2H_2$$

Typically, the residual organic matter in the SiC powder was removed through being calcined in a muffle furnace at 650 ^oC for 3 h. Then, 6 g pre-treated 3C-SiC powder (40 nm) was added in an etching solution consisting of 15 mL nitric acid (HNO_3, 65 wt.%) and 45 mL hydrofluoric acid (HF, 40 wt.%). The above mixed solution was put into an oil bath for etching at 100 °C for 1 h. After naturally cooling, the solution was centrifuged at 10,000 rpm for 10 min to remove excess acid. The precipitation was washed several times with deionized water and ethanol, then dispersed in 30 mL deionized water under sonication for 60 min. The supernatant of ultrasmall SiC NCs was collected by centrifugation at 7,500 rpm for 10 min. The concentration was adjusted to 1 mg/mL.

The preparation of CN/SiC NCs composite

CN/SiC NCs composite was prepared by a hydrothermal method. Firstly, 100 mg of CN was added to a certain volume of deionized water, and different volumes (5, 10, 15, 20 mL) of 3C-SiC nanocrystal solution (1 mg/mL) were added sequentially, and the total volume was fixed at 40 mL. Then the mixed solution was ice bath ultrasound for 1 h and followed by stirring for 4 h. Subsequently, the solution obtained above was transferred to a 50 mL Teflon-lined stainless-steel autoclave and heated at 120 °C for 10 h. After that, the obtained composite was washed several times with deionized water and ethanol, and dried in a vacuum drying oven at 60 °C to get the CN/SiC NCs composites. The composites containing different mass fractions of SiC NCs were denoted as CN/SiC NCs-5, CN/SiC NCs-10, CN/SiC NCs-15, and CN/SiC NCs-20, respectively. A diagram of synthesizing CN, SiC NCs and CN/SiC NCs is shown in Fig. S1.

Characterizations

X-ray diffraction (XRD) patterns were examined by a Bruker D8 advance diffractometer using Cu Kα radiation in the 2θ range from 5° to 80°. The morphologies and microstructures of the

samples were characterized by a scanning electron microscope (SEM, JEOL, JSM-6700F, Japan) and a transmission electron microscope (TEM, JEOL, JEM-2100PLUS, Japan). Photoluminescence (PL) measurements were conducted on a PL spectrometer (FLS100, Edinburgh). A 375 nm picosecond pulsed laser was used as the excitation source for time resolved PL measurements. X-ray photoelectron spectroscopy (XPS) was used to analyze the structure and composition of the samples by Thermo ESCALAB 250Xi with Al Kα source. The XPS spectra were calibrated through the standard C1s peak at 284.6 eV. UV-Vis spectra in the range of 200-800 nm were recorded by a spectrophotometer (Cary 5000, Varian, USA, $BaSO_4$ was used as a reflectance standard).

Photoelectrochemical measurements

An electrochemical analyzer (Autolab, PGSTAT 302N) with a standard three-electrode system was used to perform electrochemical measurements. 0.1 M Na_2SO_4 solution was used as the electrolyte for transient photocurrent (IT) and electrochemical impedance spectroscopy (EIS), and 0.1 M KOH solution as the electrolyte for linear sweep voltammetry (LSV) tests. The catalyst was coated on FTO glass with a light irradiation area of 1 cm^2 as the working electrode of the three-electrode system, the platinum sheet and Ag/AgCl were used as the counter electrode and the reference electrode, respectively. Typically, 5 mg of catalyst was dispersed in 280 μL deionized water, after sonication 20 μL of Nafion solution was added to form a uniform suspension, which was then uniformly dropped on the FTO glass and dried on the heating plate to ensure that the sample was tightly attached onto the FTO substrate. The EIS was carried out in the frequency range from 0.01 Hz to 100 kHz with an ac amplitude of 100 mV. Transient photocurrent (I-t) was tested at a 0.8 V bias. The LSV scan rate was 10 mV s^{-1} in dark or with light irradiation (300 W Xe lamp, 1.5 AM filter).

Photocatalytic hydrogen production

Photocatalytic water splitting reaction over the photocatalysts was conducted in a pyrex top-

irradiation reaction vessel connected to a closed glass gas circulation system (CEL-SPH2N, Beijing China Education Au-light Co. Ltd., China), with cooling water to maintain the reaction solution at room temperature. Briefly, 20 mg of photocatalyst powders (CN, CN/SiC NCs) were dispersed in 100 mL aqueous solution containing 10 vol.% triethylamine scavengers (90 mL water and 10 mL TEOA) and 3 wt.% (relative to Pt) $H_2PtCl_6 \cdot 6H_2O$ as a cocatalyst. The solution was controlled below 6 °C through a cooling water device during the whole experiment. Before the test, the prepared suspension was evacuated for 20 min to remove air completely and to ensure that the reaction was under vacuum. A 300 W Xe lamp with a 420 nm cut-off filter was used as visible light source. The amount of hydrogen evolution was analyzed by a gas chromatographer (GC7920, Beijing China Education Au-light Co. Ltd., China), the high-purity N_2 (99.999%) was used as the carrier gas. The rate of hydrogen production was calculated as follows:

$$Hydrogen\ production\ (\mu mol/(g \cdot h)) = \frac{C}{22.4 \times m} \times 10^6$$

Where C is the volume of hydrogen production per hour (L/h) and m is the quantity of the photocatalyst (g).

The apparent quantum yield (AQY) for hydrogen evolution was measured under illumination of the simulated solar light with a band-pass filter (420 ± 5 nm). Photon flux of the incident light was measured using an optical power meter (CEL-NP2000, Beijing China Education Au-Light Co., Ltd). Photocatalytic reaction was kept for 5 h and the moles of hydrogen produced per hour was calculated to be $7.73 \times 10^{-5}\ mol/h$. The AQY is calculated according to the following equation:

$$AQY(\%) = \frac{N_e}{N_p} = \frac{2 \times number\ of\ evolved\ H_2\ molecules}{number\ of\ incident\ photons} \times 100\%$$

$$= \frac{N_e \times h \times c}{P\ S\ t\ \lambda} \times 100\%$$

λ is the incident wavelength of monochromatic light, h is the Planck's constant, and c is the speed of light. P and S represent the intensity of the light source and the irradiated area,

respectively.

$$AQY(\%) = \frac{2 \times 7.73 \times 10^{-5} \times 6.02 \times 10^{23} \times 6.62 \times 10^{-34} \times 3.0 \times 10^{8}}{0.124 \times 3600 \times 420 \times 10^{-9}} \times 100\% = 9$$

DFT calculations

A kinetic energy cutoff of 490 eV was used to represent the single-particle wave functions. In the calculation model, water molecule was adsorbed on the Si- or C-terminated surfaces of the 3C-SiC NCs. The top layer of the model was covered with 1.0 nm thick vacuum slab. The geometric optimization was carried out by DFT calculation under the CASTEP package with convergence tolerances of 2×10^{-5} eV for energy, 0.05 eV/Å for maximum force, and 0.002 Å for maximum displacement.

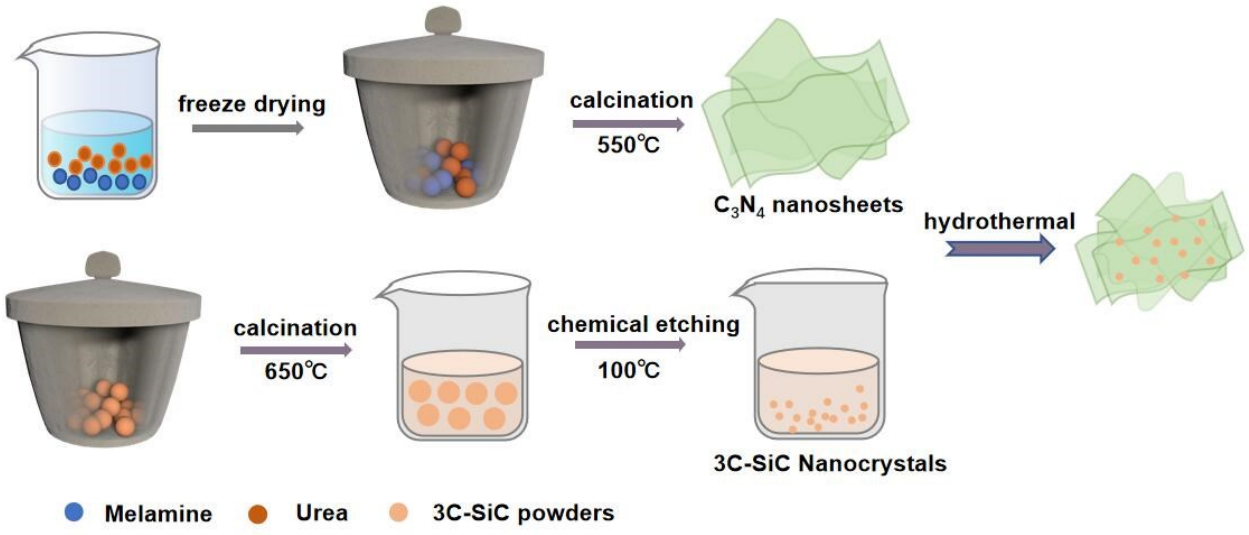

Fig S1. Schematic diagram of synthesizing CN, SiC NCs, and CN/SiC NCs.

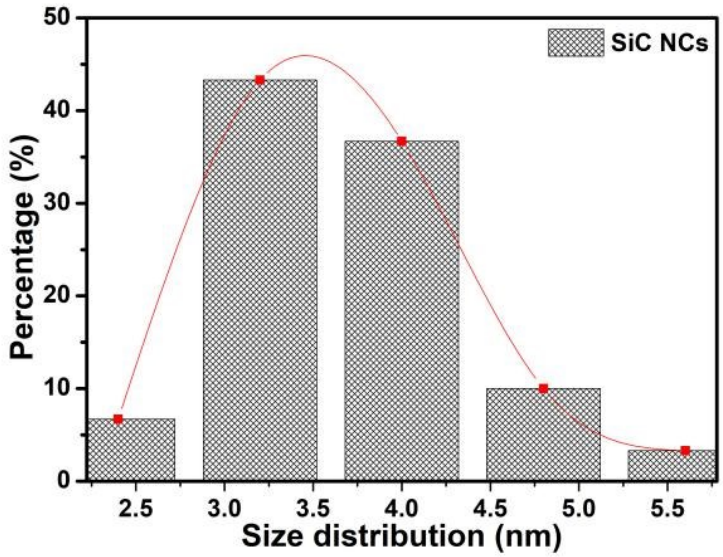

Fig S2. Size distribution of SiC nanocrystals.

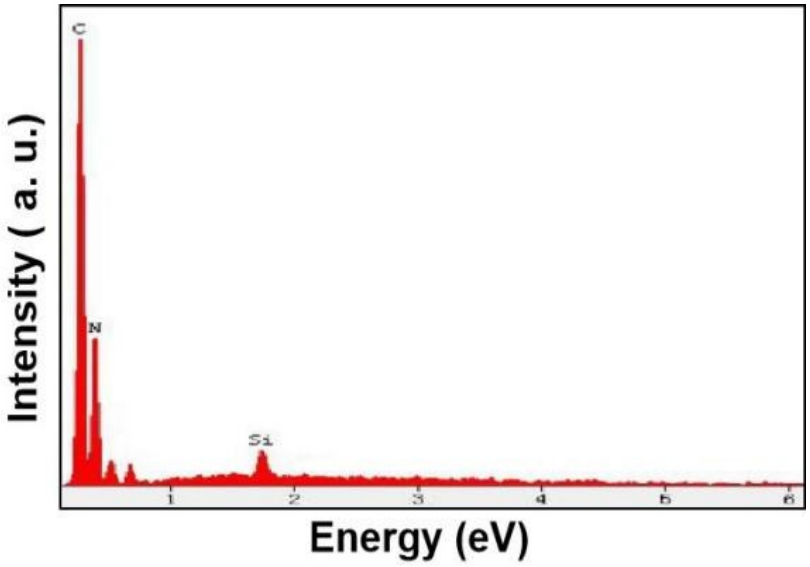

Fig. S3. EDS result of CN/SiC NCs-10.

Table S1. The surface elemental contents of CN/SiC NCs-10.

	Weight%	Atomic%
C K	36.7	40..8
N K	60.6	57.9
Si K	2.7	1.3
Totals	100.0	

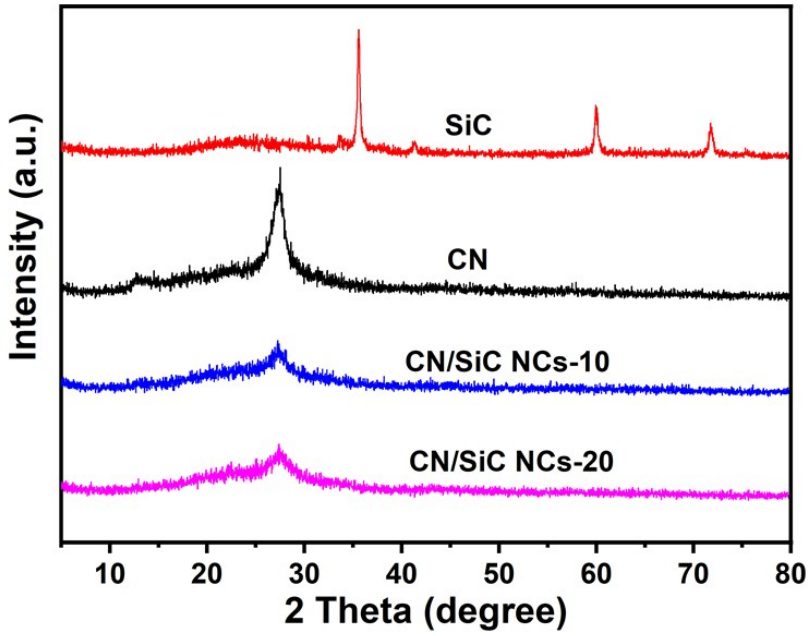

Fig. S4. XRD patterns of CN, SiC NCs, and CN/SiC NCs composites with different contents of SiC NCs.

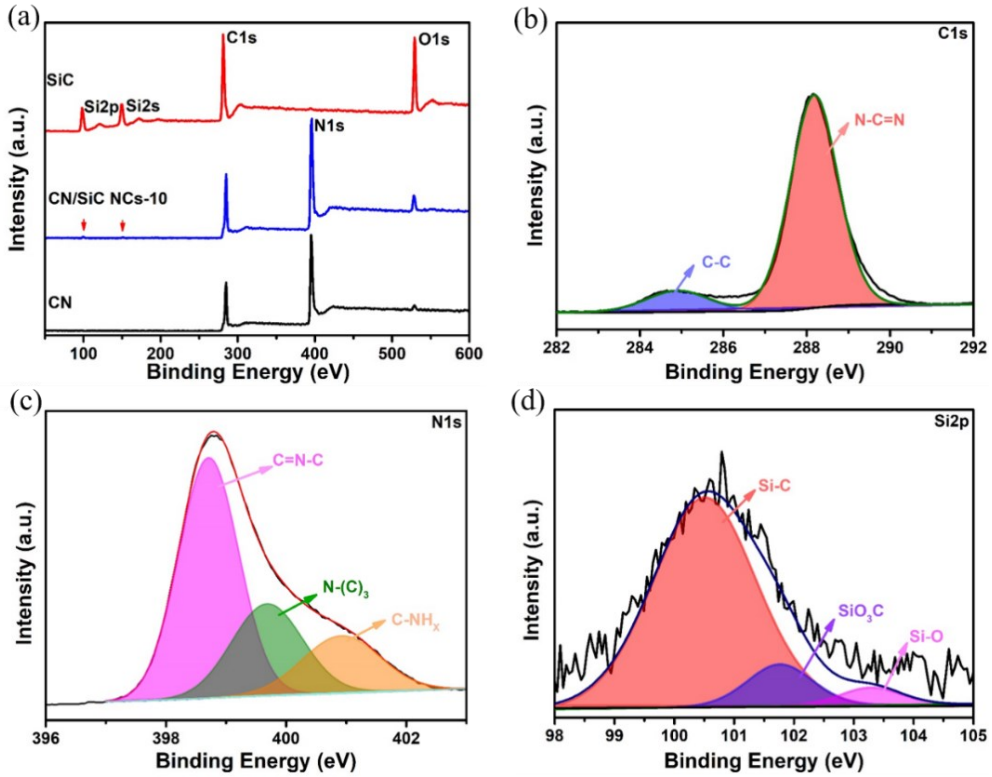

Fig. S5. (a) Full survey XPS spectra of CN, SiC NCs, CN/SiC NCs-10 composite. High-resolution XPS spectra of (b) C 1s, (c) N 1s, and (d) Si 2p of CN/SiC NCs.

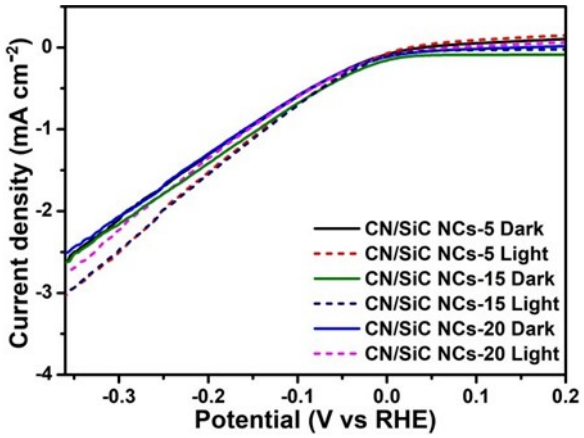

Fig. S6. Linear sweep voltammogram (LSV) measurements of CN/SiC NCs with different SiC NCs contents in dark and light condition.

Table S2. Comparison of the CN/SiC NCs with other C_3N_4 related photocatalysts.

Photocatalyst	Reaction condition	H_2 production ($\mu mol\ h^{-1}\ g^{-1}$)	AQY(%)	Ref
CN/SiC NCs	3.0wt%Pt TEOA 20 mg catalyst	1889	9.8% (420 nm)	This work
C_3N_4/SiC	1.0wt%Pt TEOA 50 mg catalyst	182	N/A	2
C_3N_4/BPQDs	3.0wt%Pt Anhydrous methanol 40 mg catalyst	271	N/A	3
P- C_3N_4	3.0wt%Pt TEOA 100 mg catalyst	1211	N/A	4
K- C_3N_4	3.0wt%Pt TEOA 30 mg catalyst	919.5	6.98% (420 nm)	5
C_3N_4/BCNQDs	1.5wt%Pt TEOA 50 mg catalyst	1401	10.0% (420 nm)	6
U-CN	3.0wt%Pt TEOA 50 mg catalyst	812	N/A	7
Se-CNs	3.0wt%Pt TEOA 25 mg catalyst	2555	1.69% (420 nm)	8
Ni_2P QDs/C_3N_4	3.0wt%Pt TEOA 20 mg catalyst	1503	4.8% (400 nm)	9
NiS_2 QDs/C_3N_4	TEOA 5 mg catalyst	968.2	2% (425 nm)	10
CoP/C_3N_4	TEOA 10 mg catalyst	1074	6.1% (420 nm)	11
CdS QDs/C_3N_4	0.5wt%Pt L-ascorbic acid 5 mg catalyst	4494	8.0% (420 nm)	12
S,N-CDs/C_3N_4	Na_2S/Na_2SO_3 1 mg catalyst	832	3.47% (460 nm)	13

P-DCN	3.0wt%Pt TEOA 10mg catalyst	2090	1.46% (420 nm)	14
$CdS/WS_2/g\text{-}C_3N_4$	TEOA 10 mg catalyst	1174.5	5.4% (420 nm)	15
F8BT Pdots/CNUS	TEOA 20 mg catalyst	929.3	5.7% (420 nm)	16
$Ag/CQDs/C_3N_4$	TEOA 5 mg catalyst	626.93	4.81% (400 nm)	17
FeP/C_3N_4	TEOA 60 mg catalyst	177.9	1.57% (420 nm)	18
CQDs/CNNS	TEOA 10 mg catalyst	219.5	1.4% (405 nm)	19
$S\text{-}C_3N_4$	3.0wt%Pt TEOA 10mg catalyst	1360	5.8% (440 nm)	20

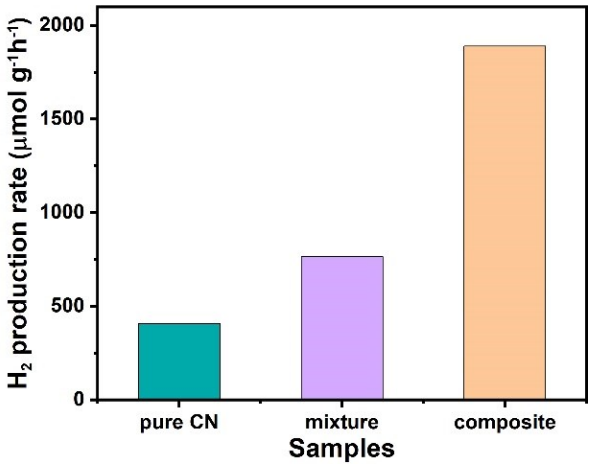

Fig. S7. Photocatalytic H_2 evolution rates of CN, CN-SiC NCs mixture, and CN/SiC NCs-10 composite.

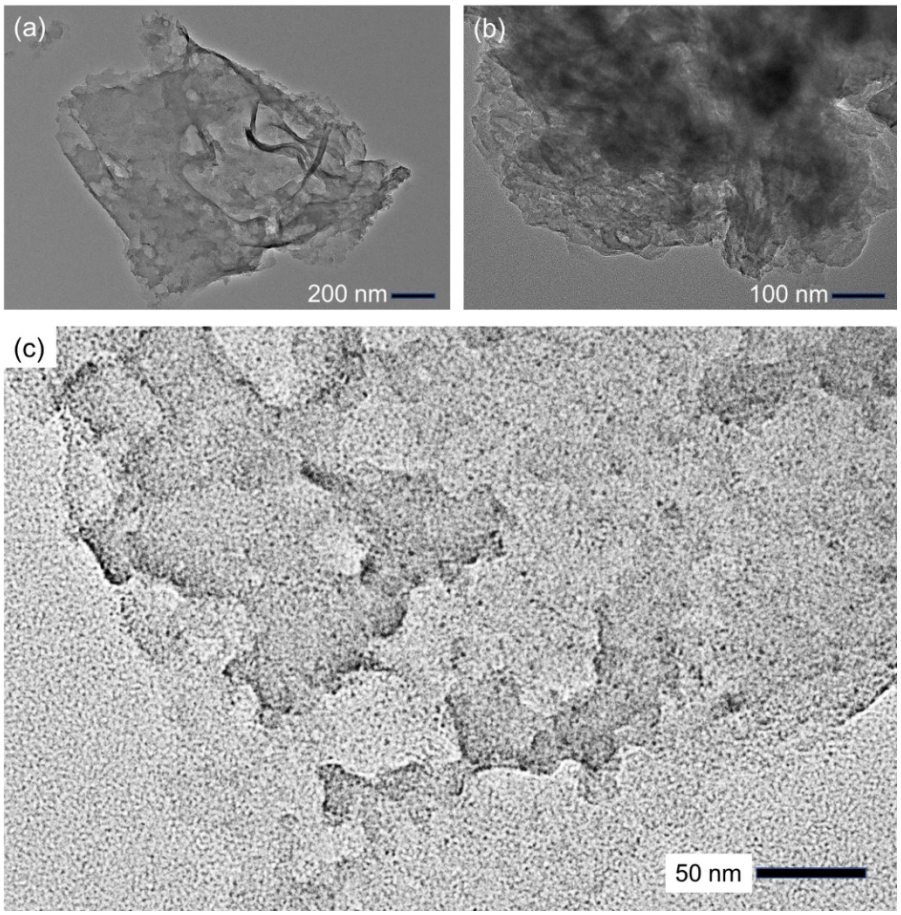

Fig. S8. TEM images of CN/SiC NCs-10 after photocatalytic test captured at different magnifications.

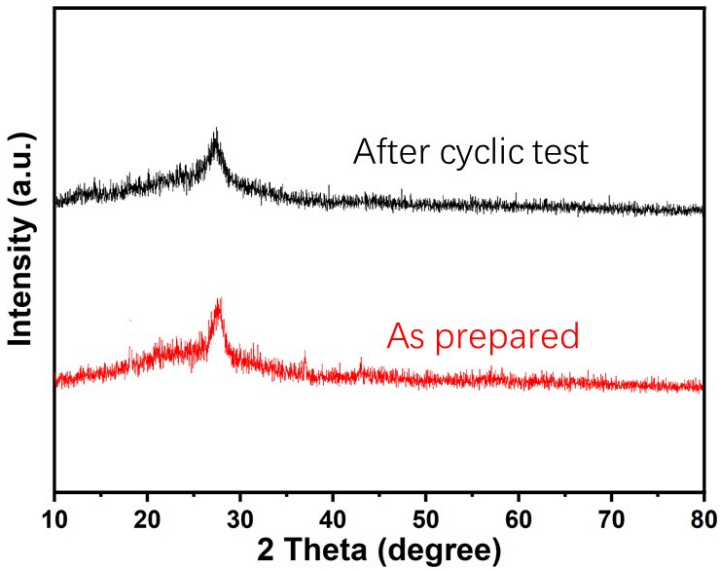

Fig. S9. XRD patterns of as-prepared CN/SiC NCs-10 and CN/SiC NCs -10 after photocatalytic test.

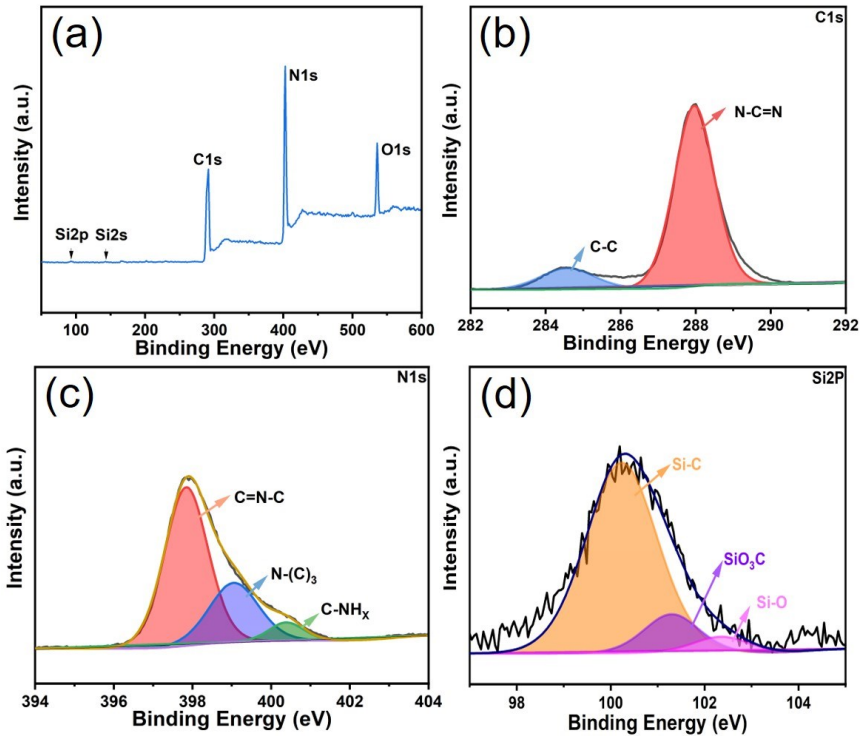

Fig. S10. XPS spectra of CN/SiC NCs-10 after photocatalytic test. (a) Full survey XPS spectrum, (b) C 1s spectrum, (c) N 1s spectrum, and (d) Si 2p spectrum.

SI reference

1. J. Zhu, Z. Liu, X. L. Wu, L. L. Xu, W. C. Zhang and P. K. Chu, *Nanotechnology*, 2007, **18**, 365603.
2. B. Wang, J. Zhang and F. Huang, *Appl. Surf. Sci.*, 2017, **391**, 449-456.
3. W. Lei, Y. Mi, R. Feng, P. Liu, S. Hu, J. Yu, X. Liu, J. A. Rodriguez, J.-O. Wang, L. Zheng, K. Tang, S. Zhu, G. Liu and M. Liu, *Nano. Energy.*, 2018, **50**, 552-561.
4. Z. Zhao, C. Xie, H. Cui, Q. Wang, Z. Shu, J. Zhou and T. Li, *Diamond Relat. Mater.*, 2020, **104**, 107734.
5. S. Sun, J. Li, J. Cui, X. Gou, Q. Yang, Y. Jiang, S. Liang and Z. Yang, *Int. J. Hydrogen Energy*, 2019, **44**, 778-787.
6. Y. Wang, Y. Li, J. Zhao, J. Wang and Z. Li, *Int. J. Hydrogen Energy*, 2019, **44**, 618-628.
7. C. Dong, Z. Ma, R. Qie, X. Guo, C. Li, R. Wang, Y. Shi, B. Dai and X. Jia, *Appl. Catal., B*, 2017, **217**, 629-636.
8. Y. Zhang, Y. Wang, M. Di, B. Zhou, W. Xu, N. Wu, Y. Wu, Y. Du and W. Zhong, *Chem. Eng. J.*, 2020, **385**, 123938.
9. Z. Lu, C. Li, J. Han, L. Wang, S. Wang, L. Ni and Y. Wang, *Appl. Catal., B*, 2018, **237**, 919-926.
10. F. Xue, M. Liu, C. Cheng, J. Deng and J. Shi, *ChemCatChem*, 2018, **10**, 5441-5448.
11. B. Luo, R. Song, J. Geng, X. Liu, D. Jing, M. Wang and C. Cheng, *Appl. Catal., B*, 2019, **256**, 117819.
12. S.-W. Cao, Y.-P. Yuan, J. Fang, M. M. Shahjamali, F. Y. C. Boey, J. Barber, S. C. Joachim Loo and C. Xue, *Int. J. Hydrogen Energy*, 2013, **38**, 1258-1266.
13. Z. Xie, S. Yu, X.-B. Fan, S. Wei, L. Yu, Y. Zhong, X.-W. Gao, F. Wu and Y. Zhou, *Journal of Energy Chemistry*, 2021, **52**, 234-242.
14. D. Zhang, Y. Guo and Z. Zhao, *Appl. Catal., B*, 2018, **226**, 1-9.
15. Y. Zou, J. W. Shi, D. Ma, Z. Fan, L. Cheng, D. Sun, Z. Wang and C. Niu, *ChemSusChem*, 2018, **11**, 1187-1197.
16. W. Zhou, T. Jia, H. Shi, D. Yu, W. Hong and X. Chen, *J. Mater. Chem. A*, 2019, **7**, 303-311.
17. J. Qin and H. Zeng, *Appl. Catal., B*, 2017, **209**, 161-173.
18. D. Zeng, T. Zhou, W. J. Ong, M. Wu, X. Duan, W. Xu, Y. Chen, Y. A. Zhu and D. L. Peng, *ACS Appl Mater Interfaces*, 2019, **11**, 5651-5660.
19. X. Xia, N. Deng, G. Cui, J. Xie, X. Shi, Y. Zhao, Q. Wang, W. Wang and B. Tang, *Chem. Commun.*, 2015, **51**, 10899-10902.
20. J. Hong, X. Xia, Y. Wang and R. Xu, *J. Mater. Chem.*, 2012, **22**, 15006.